

Pentanuclear Homoleptic M_5L_6 ($M = Mn(II), Co(II), Zn(II)$) Complexes Formed by Strict Self-Assembly

Craig J. Matthews,^{†,‡} Laurence K. Thompson,^{*,†} Stewart R. Parsons,[†] Zhiqiang Xu,[†] David O. Miller,[†] and Sarah L. Heath[§]

Department of Chemistry, Memorial University, St. John's, Newfoundland, A1B 3X7, Canada, and Department of Chemistry, University of York, Heslington, York, YO10 5DD, UK

Received March 19, 2001

A series of trigonal bipyramidal pentanuclear complexes involving the alkoxo-diazine ligands poap and p3oap, containing the $M_5[\mu-O]_6$ core is described, which form by a strict self-assembly process. $[Co_5(poap-H)_6](ClO_4)_4 \cdot 3H_2O$ (**1**), $[Mn_5(poap-H)_6](ClO_4)_4 \cdot 3.5CH_3OH \cdot H_2O$ (**2**), $[Mn_5(p3oap-H)_6](ClO_4)_4 \cdot CH_3CH_2OH \cdot 3H_2O$ (**3**), and $[Zn_5(poap-H)_6](ClO_4)_4 \cdot 2.5H_2O$ (**4**) are homoleptic pentanuclear complexes, where there is an exact match between the coordination requirements of the five metal ions in the cluster, and the available coordination pockets in the polytopic ligand. $[Zn_4(poap)(poap-H)_3(H_2O)_4](NO_3)_5 \cdot 1.5H_2O$ (**5**) is a square $[2 \times 2]$ grid with a $Zn_4[\mu-O]_4$ core, and appears to result from the presence of NO_3 , which is thought to be a competing ligand in the self-assembly. X-ray structures are reported for **1**, **4**, and **5**. **1** crystallized in the monoclinic system, space group $P2_1/n$ with $a = 13.385(1)$ Å, $b = 25.797(2)$ Å, $c = 28.513(3)$ Å, $\beta = 98.704(2)^\circ$, and $Z = 4$. **4** crystallized in the triclinic system, space group $P\bar{1}$ with $a = 13.0897(9)$ Å, $b = 18.889(1)$ Å, $c = 20.506(2)$ Å, $\alpha = 87.116(1)^\circ$, $\beta = 74.280(2)^\circ$, $\gamma = 75.809(2)^\circ$, and $Z = 2$. **5** crystallized in the monoclinic system, space group $P2_1/n$ with $a = 14.8222(7)$ Å, $b = 21.408(1)$ Å, $c = 21.6197(9)$ Å, $\beta = 90.698(1)^\circ$, and $Z = 4$. Compounds **1–3** exhibit intramolecular antiferromagnetic coupling.

Introduction

Self-assembly reactions are a key strategic tool for the synthesis of supramolecular materials, and specific ligand design strategies, based on the concept of appropriately positioned coordination pockets, can lead to single, high nuclearity components, in high yield. If the pockets form a contiguous linear array the outcome of the self-assembly process can lead to grids, with the possibility of significant magnetic exchange between adjacent paramagnetic metal centers if appropriate bridging groups are included. This approach has an advantage in that ligand design features can be pre-programmed into a system to generate a polynuclear system of a specific size, and possibly with tailored magnetic properties.

Aromatic polytopic diazine ligands with central bridging pyridazine,¹ pyrimidine,^{2–5} tetrazine,⁶ pyrazolate,⁷ and open

chain diazine (N–N)⁸ cores have been successfully used to generate tetranuclear square grids with such metal ions as Cu(I), Co(II), Ni(II) and Cu(II). Antiferromagnetic coupling was observed within the grids for the $M_4(\text{pyrimidine})_4$ ($M = Co(II), Ni(II)$),^{3,4} $Ni(II)_4(\text{tetrazine})_4$ ⁶ and $Cu(II)_4(\text{pyrazolate})_4$ ⁷ systems, with an essentially uncoupled situation for $Cu(II)_4(N-N)_4$.⁸ An unusual $Co(II)_4S_4$ square grid results from the reaction of tetrapyrrolylthiocarbazonate with $CoCl_2$, but no magnetic data were reported.⁹

A key element in the rationale synthesis of spin coupled clusters is the choice of a viable superexchange bridge, and the judicious positioning of the bridge in the polytopic ligand framework. Flexible diazine ligands containing an alcohol fragment (Scheme 1) have two potentially bridging groups (alkoxide and diazine) and have been shown to successfully self-assemble square $M(II)_4[\mu-O]_4$ grids in high yield with Cu(II), Ni(II), Mn(II), and Co(II) salts.^{10,11} The $Mn(II)_4$, $Co(II)_4$, and $Ni(II)_4$ squares exhibit antiferromagnetic coupling, consistent with the large M–O–M bridge angles, while the exchange in the $Cu(II)_4$ systems is always dominated by ferromagnetic coupling as a result of strict orthogonality of the metal magnetic orbitals in the grid, despite large Cu–O–Cu bridge angles.

Higher homologous grids, e.g. Ag_6 , can be produced by combining ligands with single and double pyridazine bridges,¹²

* To whom correspondence should be addressed. E-mail: lthomp@mun.ca. Fax: 709-737-3702.

† Memorial University.

‡ University of York.

§ Present address: Department of Chemistry and Physics, The Nottingham Trent University, Clifton Lane, Nottingham, NG11 8NS, UK.

- (1) Youinou, M.-T.; Rahmouni, N.; Fischer, J.; Osborn, J. A. *Angew. Chem., Int. Ed. Engl.* **1992**, *31*, 733.
- (2) Hanan, G. S.; Volkmer, D.; Ulrich, S. S.; Lehn, J.-M.; Baum, G.; Fenske, D. *Angew. Chem., Int. Ed. Engl.* **1997**, *36*, 1842.
- (3) Waldmann, O.; Hassmann, J.; Müller, P.; Hanan, G. S.; Volkmer, D.; Schubert, U. S.; Lehn, J.-M. *Phys. Rev. Lett.* **1997**, *78*, 3390.
- (4) Waldmann, O.; Hassmann, J.; Müller, P.; Volkmer, D.; Schubert, U. S.; Lehn, J.-M. *Phys. Rev. B* **1998**, *58*, 3277.
- (5) Bassani, D. M.; Lehn, J.-M.; Fromm, K.; Fenske, D. *Angew. Chem., Int. Ed. Engl.* **1998**, *37*, 2364.
- (6) Campos-Fernández, C. S.; Clérac, R.; Dunbar, K. R. *Angew. Chem., Int. Ed. Engl.* **1999**, *38*, 3477.
- (7) Mann, K. L. V.; Psillakis, E.; Jeffery, J. C.; Rees, L. H.; Harden, N. M.; McCleverty, J. A.; Ward, M. D.; Gatteschi, D.; Totti, F.; Mabbs, F.; McInnes, E. J. L.; Riedi, P. C.; Smith, G. M. *J. Chem. Soc., Dalton Trans.* **1999**, 339.

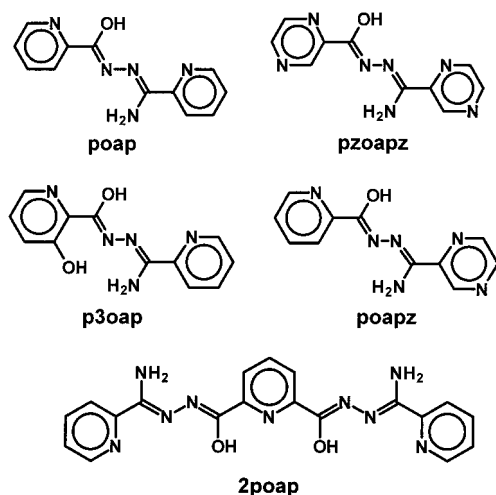
(8) Van Koningsbruggen, P. J.; Müller, E.; Haasnoot, J. G.; Reedijk, J. *Inorg. Chim. Acta* **1993**, *208*, 37.

(9) Duan, C.-y.; Liu, Z.-h.; You, X.-z.; Xue, F.; Mak, T. C. W. *Chem. Commun.* **1997**, 381.

(10) Matthews, C. J.; Avery, K.; Xu, Z.; Thompson, L. K.; Zhao, L.; Miller, D. O.; Biradha, K.; Poirier, K.; Zaworotko, M. J.; Wilson, C.; Goeta, A. E.; Howard, J. A. K. *Inorg. Chem.* **1999**, *38*, 5266.

(11) Thompson, L. K.; Matthews, C. J.; Zhao, L.; Xu, Z.; Miller, D. O.; Wilson, C.; Leech, M. A.; Howard, J. A. K.; Whittaker, G. A.; Winpenny, R. E. P. *J. Solid State Chem.* **2001**, *159*, 308.

Scheme 1



and with the double pyridazine ligand alone self-assembly produces a remarkable $Ag_9(\text{pyridazine})_{12}$ square grid.¹³ Of major significance in the quest for *magnetic* grids are the recent reports of an antiferromagnetically coupled $Mn(II)_9$ grid,¹⁴ and a ferromagnetically coupled $Cu(II)_9$ grid¹⁵ with the ligand 2poap (Scheme 1). In these systems six ligands and nine metals self-assemble in high yield into a $M_9[\mu-O]_{12}$ square interlocking grid, with large $M-O-M$ angles. Magnetic orbital orthogonality in the $Cu_9[\mu-O]_{12}$ grid leads to dominant intramolecular ferromagnetic coupling and a $S = 7/2$ ground state.^{15,16}

The choice of an ultimate cluster size in a self-assembly process depends on a number of factors, but metal ion coordination number and geometric preference are key elements, in addition to the size and arrangement of the ligand coordination pockets. The tetradentate ligands such as poap (Scheme 1) produce square grids with copper(II) salts in all cases, seemingly irrespective of the anion. Each ligand fills five metal coordination sites because the deprotonated alkoxo-oxygen acts as a bridge.¹⁰ This seems to be true also in the nickel system.¹⁰ However with $Mn(II)$ there appears to be a preferred choice of the cluster outcome, dependent upon the identity of the anion. With $Mn(\text{ClO}_4)_2$ a novel homoleptic trigonal bipyramidal cluster, $[Mn_5(\text{poap-H})_6](\text{ClO}_4)_4$, results. Some structural details of this compound have already been reported.¹⁷ In this system there is an exact match between the coordination requirements of the five octahedral metal ions and the coordination pocket arrangement of the six ligands. However with other salts e.g. nitrate, a square tetranuclear $Mn_4[\mu-O]_4$ grid results.¹¹ This report details the synthesis, structural, and magnetic study of examples of new homoleptic trigonal-bipyramidal $M_5[\mu-O]_6$ clusters ($M = Mn(II)$, $Co(II)$, and $Zn(II)$) involving the ligand poap, all with perchlorate anions, and a $Zn_4[\mu-O]_4$ square grid with $Zn(\text{NO}_3)_2$.

Experimental Section

Physical Measurements. Infrared spectra were recorded as Nujol mulls using a Mattson Polaris FT-IR instrument. Microanalyses were carried out by Canadian Microanalytical Service, Delta, Canada.

- (12) Baxter, P. N. W.; Lehn, J.-M.; Kneisel, B. O.; Fenske, D. *Angew. Chem., Int. Ed. Engl.* **1997**, *36*, 1978.
 (13) Baxter, P. N. W.; Lehn, J.-M.; Fischer, J.; Youinou, M.-T. *Angew. Chem., Int. Ed. Engl.* **1994**, *33*, 2284.
 (14) Zhao, L.; Matthews, C. J.; Thompson, L. K.; Heath, S. L. *Chem. Commun.* **2000**, 265.
 (15) Zhao, L.; Xu, Z.; Thompson, L. K.; Heath, S. L.; Miller, D. O.; Ohba, M. *Angew. Chem., Int. Ed.* **2000**, *39*, 3114.
 (16) Waldmann, O.; Koch, P.; Schromm, S.; Müller, P.; Zhao, L.; Thompson, L. K. *Chem. Phys. Lett.* **2000**, *332*, 73.
 (17) Matthews, C. J.; Xu, Z.; Mandal, S. K.; Thompson, L. K.; Biradha, K.; Poirier, K.; Zaworotko, M. J. *Chem. Commun.* **1999**, 347.

Variable temperature magnetic data (2–300K) were obtained using a Quantum Design MPMS55 SQUID magnetometer with field strengths of 0.1–5.0 T. Samples were prepared in gelatin capsules or aluminum cups, mounted inside straws. Background corrections for the sample holder assembly, and diamagnetic components of the complexes were applied.

Synthesis of Ligands and Complexes. Poap was synthesized by a published procedure.^{10,18} p3oap was synthesized according to the following general procedure.

The methyl ester of imino-picolinic acid was prepared in situ by reaction of 2-cyanopyridine (6.2 g, 60 mmol) with sodium methoxide solution, produced by dissolving sodium metal (0.14 g, 6.1 mmol) in dry methanol (75 mL). The carboxylic acid hydrazide (7.5 g, 50 mmol) (prepared from the reaction of methyl-3-hydroxy-2-pyridinecarboxylate with hydrazine hydrate in methanol) was added to the above solution and the mixture gently refluxed for 3 h. A yellow precipitate formed, which was filtered off, washed with methanol, diethyl ether, and dried under vacuum. Yield: p3oap (72%) (mp 268 °C (dec)). Mass spectrum (major mass peaks, m/z): 257(M), 239 (M–H₂O), 223, 183, 163, 107. IR (Nujol mull, cm^{-1}): 3287 (OH, νNH_2) (m); 1688 (s) ($\nu\text{C}=\text{O}$); 1650 (s) ($\nu\text{C}=\text{N}$); 1000 (m) (vpy). Anal. Calcd for $C_{12}H_{11}N_5O_2 \cdot 3H_2O$: C, 46.29; H, 5.46; N, 22.50. Found: C, 46.28; H, 4.90; N, 22.27.

[Co₅(poap-H)₆](ClO₄)₄·3H₂O (1). Poap (1.0 mmol) was added to a hot stirred solution of $Co(\text{ClO}_4)_2 \cdot 6H_2O$ (1.0 mmol) in water (20 mL). The ligand dissolved slowly, and then a pale orange precipitate formed, which was filtered off, washed with ethanol and ether, and dried under vacuum (Yield 75%). The product was recrystallized from acetonitrile by ether diffusion to give dark orange crystals suitable for X-ray analysis. The crystals lose solvent on exposure to air, and were kept under mother liquor prior to structural analysis. Recrystallization from other solvents in the presence of air produced dark brown solids, suggesting oxidation. A sample was vacuum-dried for elemental analysis and magnetic measurements. Anal. Calcd for $[Co_5(C_{12}H_{10}N_5O)_6](\text{ClO}_4)_4 \cdot 3H_2O$: C, 39.52; H, 3.02; N, 19.21. Found: C, 39.58; H, 2.81; N, 19.43. Some lattice solvent molecules, which have been shown to be present in the X-ray structure (CH_3CN , H_2O) (vide infra), are lost on vacuum-drying.

[Mn₅(p3oap-H)₆](ClO₄)₄·CH₃CH₂OH·3H₂O (3). This compound was prepared in a manner similar to **1** in a water/methanol mixture using $Mn(\text{ClO}_4)_2 \cdot 6H_2O$ and p3oap, to give an orange colored solid, followed by recrystallization from a methanol/ethanol (50/50) mixture to give orange crystals suitable for structural analysis (Yield 55%). Anal. Calcd for $[Mn_5(C_{12}H_{10}N_5O)_6](\text{ClO}_4)_4 \cdot \text{CH}_3\text{CH}_2\text{OH} \cdot 3H_2O$: C, 38.47; H, 3.12; N, 18.19. Found: C, 38.34; H, 2.87; N, 18.21.

[Zn₅(poap-H)₆](ClO₄)₄·2.5H₂O (4). Compound **4** was prepared by adding poap (1.0 mmol) to a warm aqueous solution (20 mL) of $Zn(\text{ClO}_4)_2 \cdot 6H_2O$ (1.0 mmol). The yellow precipitate which formed was filtered off, washed with ethanol and ether, dried, and recrystallized from MeCN/Water (4:1) to give yellow crystals suitable for structural analysis (Yield 65%). Anal. Calcd for $[Zn_5(C_{12}H_{10}N_5O)_6](\text{ClO}_4)_4 \cdot 2.5H_2O$: C, 39.11; H, 2.94; N, 19.01. Found: C, 39.12; H, 2.87; N, 19.24.

[Zn₄(poap)(poap-H)₃(H₂O)₄](NO₃)₅·1.5H₂O (5). Poap (1.0 mmol) was added to a solution of $Zn(\text{NO}_3)_2 \cdot 6H_2O$ (1.0 mmol) in water (20 mL). The mixture was stirred with heating for 5 min. forming a clear yellow solution. The solution was filtered and allowed to stand at room temperature. Yellow block shaped crystals, suitable for structural determination, were obtained after three weeks (Yield 60%). Anal. Calcd for $[Zn_4(C_{12}H_{10}N_5O)_3(C_{12}H_{11}N_5O)](\text{NO}_3)_5 \cdot 1.5H_2O$: C, 35.33; H, 3.15; N, 21.46. Found: C, 35.32; H, 3.00; N, 21.43. Some lattice water molecules, shown to be present in the X-ray structure (vide infra), are lost on vacuum-drying.

Crystallography. The diffraction intensities of an orange-red prismatic crystal of **1** were collected with graphite-monochromatized Mo K α X-radiation (rotating anode generator) using a Bruker P4/CCD diffractometer at 193(1) K to a maximum 2θ value of 51.5°. The data were corrected for Lorentz and polarization effects. The structure was solved by direct methods.^{19,20} All atoms except hydrogens were

- (18) Xu, Z.; Thompson, L. K.; Miller, D. O.; Clase, H. J.; Howard, J. A. K.; Goeta, A. E. *Inorg. Chem.* **1998**, *37*, 3620.

Table 1. Summary of Crystallographic Data for $[\text{Co}_5(\text{poap-H})_6](\text{ClO}_4)_4 \cdot 3\text{H}_2\text{O}$ (**1**), $[\text{Zn}_5(\text{poap-H})_6](\text{ClO}_4)_4 \cdot 2.5\text{H}_2\text{O}$ (**4**), $[\text{Zn}_4(\text{poap})(\text{poap-H})_3(\text{H}_2\text{O})_4](\text{NO}_3)_5 \cdot 1.5\text{H}_2\text{O}$ (**5**)

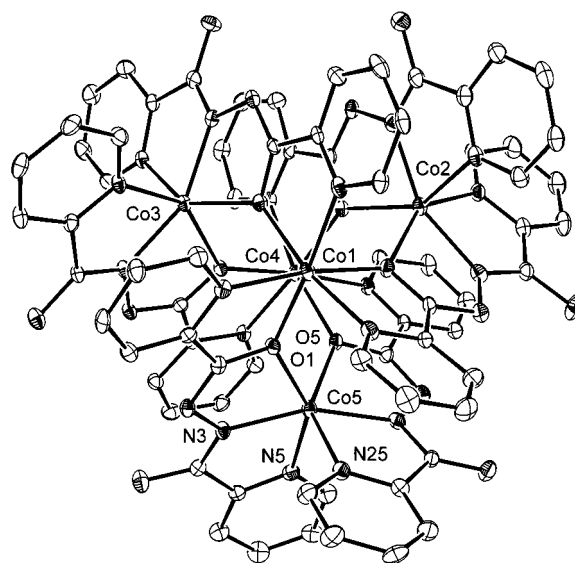
compound	1^a	4^a	5^a
empirical formula	$\text{C}_{80}\text{H}_{82}\text{N}_{34}\text{O}_{26}\text{Cl}_4\text{Co}_5$	$\text{C}_{72}\text{H}_{74}\text{N}_{30}\text{O}_{26}\text{Zn}_5\text{Cl}_4$	$\text{C}_{48}\text{H}_{65}\text{N}_{25}\text{O}_{31}\text{Zn}_4$
formula wt	2372.22	2292.27	1749.71
space group	$P2_1/n$ (#14)	$P\bar{3}$ (#2)	$P2_1/n$ (#14)
<i>a</i> (Å)	13.385(1)	13.0897(9)	14.8222(7)
<i>b</i> (Å)	25.797(2)	18.889(1)	21.408(1)
<i>c</i> (Å)	28.513(3)	20.506(2)	21.6197(9)
α (deg)	90	87.116(1)	90
β (deg)	98.704(2)	74.280(2)	90.698(1)
γ (deg)	90	75.809(2)	90
<i>V</i> (Å ³)	9732(1)	4731.0(6)	6859.7(5)
ρ_{calcd} (gcm ⁻³)	1.619	1.609	1.694
<i>Z</i>	4	2	4
μ (mm ⁻¹)	1.038	1.455	1.489
λ (Å)	0.71073	0.71073	0.71073
<i>T</i> (K)	193(1)	193(1)	193(1)
<i>R</i> 1 ^a	0.068	0.065	0.045
<i>wR</i> 2 ^b	0.201	0.194	0.143

$$^a R1 = \sum ||F_o| - |F_c|| / \sum |F_o|. \quad ^b wR2 = [\sum [w(|F_o|^2 - |F_c|^2)^2] / \sum [w(|F_o|^2)^2]]^{1/2}.$$

refined anisotropically. Hydrogen atoms were placed in calculated positions. Neutral atom scattering factors²¹ and anomalous-dispersion terms^{22,23} were taken from the usual sources. All other calculations were performed with the teXsan²⁴ crystallographic software package using a PC computer. Crystal data collection and structure refinement for **4** and **5** were carried out in a similar manner using Mo-K α radiation. Abbreviated crystal data for **1**, **4** and **5** are given in Table 1.

Diffraction data for a single crystal of **3** were collected using a Bruker SMART CCD diffractometer, equipped with an Oxford Cryostream N₂ cooling device,²⁵ with graphite monochromated Mo-K α radiation. Cell parameters were determined and refined using the SMART software,^{26a} raw frame data were integrated using the SAINT program,^{26b} and the structure was solved using Direct Methods and refined by full-matrix least squares on *F*² using SHELXTL.²⁷ Non-hydrogen atoms were refined with anisotropic atomic displacement parameters. Because of difficulties with the refinement of this structure, associated with disordered perchlorates and lattice fragments, only preliminary structural details for **3** are reported at this time.²⁸

Structures. The structure of the cation in **1** is illustrated in Figure 1, and important bond distances and angles are listed in Table 2. The overall structural arrangement shows a pentanuclear cation, four well defined perchlorate anions, four lattice acetonitrile molecules and four water molecules. The pentanuclear homoleptic cluster involves five six-

**Figure 1.** Structural representation of the cation in $[\text{Co}_5(\text{poap-H})_6](\text{ClO}_4)_4 \cdot 3\text{H}_2\text{O}$ (**1**) (20% probability thermal ellipsoids).

coordinate pseudo-octahedral cobalt(II) centers arranged at the apexes of a trigonal bipyramid, with each apical cobalt ion connected to each equatorial cobalt ion by an alkoxide bridge atom from each of the six tetradentate ligands. Each ligand actually fills five metal coordination positions because of the bridging nature of the deprotonated oxygens. Therefore there is an exact match between the donor requirements of the five metals (30 coordination sites) and available donors provided by the ligands (30). The six ligands are arranged in three groups of roughly parallel pairs around the cluster core (Figure 2), with each parallel pair arranged in opposition. The trigonal bipyramidal core, including the metal ion coordination sphere donors for the apical cobalt centers, is illustrated in Figure 3. The apical cobalt centers have *fac*-N₃O₃ chromophores, while the equatorial cobalt centers have *cis*-N₄O₂ chromophores. Cobalt–oxygen distances fall in the range 2.092–2.177 Å, and cobalt–nitrogen distances fall in the range 2.013–2.253 Å. The apical cobalt atoms (Co(1), Co(4)) have metal–ligand distances <2.14 Å, while the equatorial metals each have two long Co–N contacts >2.2 Å to the pyridine rings at the NH₂ ends of the ligands. This may be associated with the differing metal ion chromophores or steric constraints due to the wrapping of the ligands around the pentanuclear cluster. Adjacent cobalt–cobalt distances fall in the range 3.89–3.93 Å, with a separation of 4.832(2) Å between the apical metals (Co(1), Co(4)). Co–O–Co bridge angles are quite large falling in a narrow range (133.6–134.9°). The presence of four perchlorates and six ligands suggests that the cobalt ions are all in the Co(II) state (vide infra),

- (19) (a) Sheldrick, G. M. *SHELX97*; 1997. (b) SIR97: Altomare, A.; Casciarano, M.; Giacovazzo, C.; Guagliardi, A. *J. Appl. Cryst.* **1993**, *26*, 343.
- (20) DIRDIF94: Beurskens, P. T.; Admiraal, G.; Beurskens, G.; Bosman, W. P.; de Gelder, R.; Israel, R.; Smits, J. M. M. *The DIRDIF-94 program system, Technical Report of the Crystallography Laboratory, University of Nijmegen, The Netherlands*; University of Nijmegen: The Netherlands, 1994.
- (21) Cromer, D. T.; Waber, J. T. *International Tables for X-ray Crystallography*; The Kynoch Press: Birmingham, England, 1974; Vol. IV, Table 2.2 A.
- (22) Ibers, J. A.; Hamilton, W. C. *Acta Crystallogr.* **1964**, *17*, 781.
- (23) Creagh, D. C.; McAuley, W. J. *International Tables for Crystallography*; Wilson, A. J. C., Ed.; Kluwer Academic Publishers: Boston, 1992; Vol. C, Table 4.2.6.8, pp 219–222.
- (24) *teXsan for Windows: Crystal Structure Analysis Package*; Molecular Structure Corporation, 1997.
- (25) Cosier, J.; Glazer, A. M. *J. Appl. Crystallogr.* **1986**, *19*, 105.
- (26) (a) *SMART Data Collection Software*, Ver. 4.050; Siemens Analytical X-ray Instruments Inc.: Madison, WI, 1996. (b) *SAINTE Data Reduction Software*, Version 4.050; Siemens Analytical X-ray Instruments Inc.: Madison, WI, 1996.
- (27) Sheldrick, G. M. *SHELXTL 5.04/VMS, An integrated system for solving, refining and displaying crystal structures from diffraction data*. Siemens Analytical X-ray Instruments Inc.: Madison, WI, 1995.
- (28) **3** crystallized in the monoclinic system, space group $P2_1/n$ with *a* = 12.9343(18) Å, *b* = 29.527(7) Å, *c* = 25.828(3) Å, β = 98.933(10)°, and *Z* = 1. *R*₁ = 0.0906 for 9844 data (*F*_o > 4σ(*F*_o)) and *wR*₂ = 0.1413 for all data (17135).

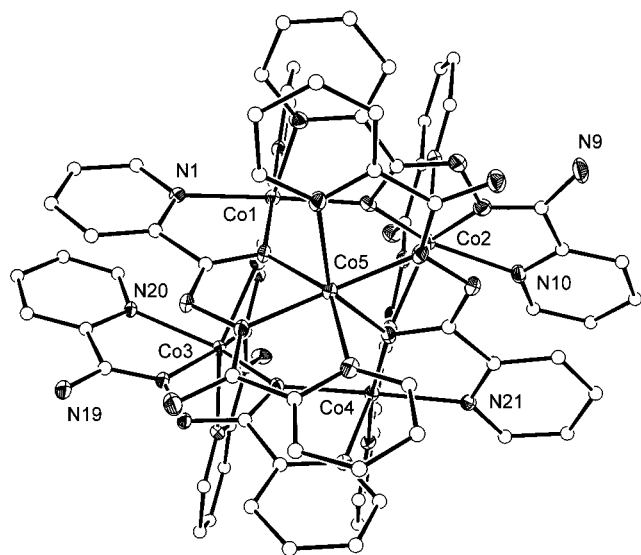
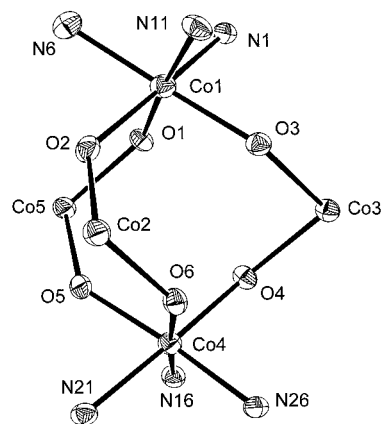
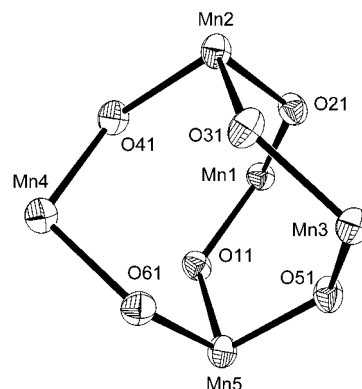
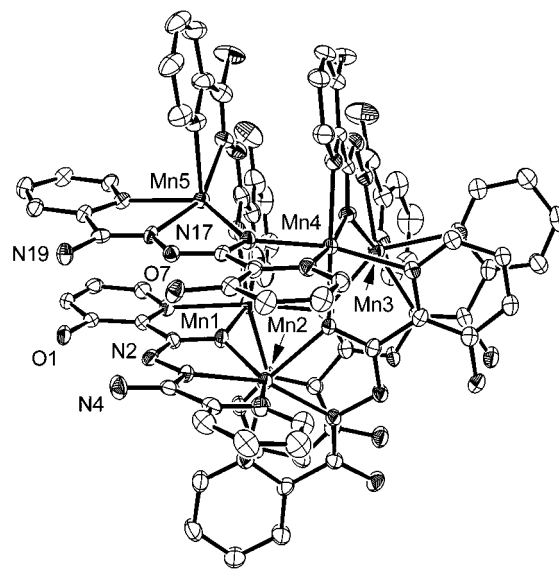
Table 2. Interatomic Distances (Å) and Angles (deg) in **1**

Co1—O1	2.076(4)	Co4—N21	2.139(5)
Co1—O2	2.107(5)	Co4—N26	2.114(5)
Co1—O3	2.108(4)	Co5—O1	2.177(4)
Co1—N1	2.108(5)	Co5—O5	2.150(4)
Co1—N6	2.114(6)	Co5—N3	2.018(5)
Co1—N11	2.138(5)	Co5—N5	2.233(6)
Co2—O2	2.131(5)	Co5—N23	2.026(6)
Co2—O6	2.154(4)	Co5—N25	2.207(5)
Co2—N8	2.025(5)	Co1—Co2	3.904(2)
Co2—N10	2.232(6)	Co1—Co3	3.906(2)
Co2—N28	2.003(5)	Co1—Co4	4.8329(2)
Co2—N30	2.227(6)	Co1—Co5	3.932(2)
Co3—O3	2.133(4)	Co4—Co5	3.920(1)
Co3—O4	2.140(4)	Co4—Co3	3.890(2)
Co3—N13	2.018(5)	Co4—Co2	3.920(2)
Co3—N15	2.249(5)	N2—N3	1.388(8)
Co3—N18	2.013(5)	N7—N8	1.402(9)
Co3—N20	2.253(5)	N12—N13	1.399(7)
Co4—O4	2.092(4)	N17—N18	1.390(8)
Co4—O5	2.095(4)	N22—N23	1.405(8)
Co4—O6	2.096(4)	N27—N28	1.392(8)
Co4—N16	2.120(5)		
Co1—O1—Co5	135.2(2)		
Co1—O2—Co2	134.2(2)		
Co1—O3—Co3	134.1(2)		
Co2—O6—Co4	134.6(2)		
Co4—O5—Co5	134.9(2)		
Co3—O4—Co4	133.6(2)		

assuming that each ligand loses one proton, a feature that is consistent with our previous observations with tetranuclear M_4 ($M = \text{Mn(II)}, \text{Co(II)}, \text{Ni(II)}, \text{Cu(II)}$) complexes of the same ligand.^{10,11}

The structure of $[\text{Mn}_5(\text{poap-H})_6](\text{ClO}_4)_4 \cdot 3.5\text{CH}_3\text{OH} \cdot \text{H}_2\text{O}$ (**2**) has been reported already,¹⁷ but some features are worthy of comment. The core trigonal bipyramidal structure is illustrated in Figure 4. Average metal–ligand distances exceed 2.20 Å for all manganese atoms, but for the equatorial metals the bonds are slightly longer (2.236–2.241 Å) than the axial ones (2.206 Å, 2.201 Å). This difference between axial and equatorial sites is less marked in **1**. Mn–O–Mn angles (128.2–130.1°) are slightly smaller than those in **1**, but the increased apical M–M separation (Mn(2)–Mn(5) 5.107(2) Å) can be attributed to the overall increased bond lengths in general. There are six very long Mn–N contacts (2.341(6)–2.403(6) Å) from the equatorial manganese centers to the NH_2 -pyridine rings, as before.

The structure of the cation in **3** is clearly resolved in the preliminary structural determination,²⁸ and is analogous to that of **2**, with an opposed arrangement of the six ligands in three roughly parallel pairs (Figure

**Figure 2.** Orientation of the structure of **1** showing the parallel arrangement of the ligands.**Figure 3.** Structural representation of the Co_5O_6 trigonal-bipyramidal core in **1**.**Figure 4.** Structural representation of the Mn_5O_6 core in $[\text{Mn}_5(\text{poap-H})_6](\text{ClO}_4)_4 \cdot 3.5\text{CH}_3\text{OH} \cdot \text{H}_2\text{O}$ (**2**).**Figure 5.** Preliminary structural representation of the cation in $[\text{Mn}_5(\text{p3oap-H})_6](\text{ClO}_4)_4 \cdot \text{CH}_3\text{CH}_2\text{OH} \cdot 3\text{H}_2\text{O}$ (**3**) (40% probability thermal ellipsoids).

5). The ligands wrap around the cluster with the amino-pyridine rings bonded to the equatorial manganese atoms, while the hydroxy-pyridine rings are all bonded to the axial manganese centers. This is the same relative arrangement as that found in **2**. Mn–Mn, Mn–N distances and Mn–O–Mn angles are close to those observed for **2**. One aspect of the structure highlights the strategy of incorporating additional donor fragments into the peripheral ligand groups, such that additional metal centers can be attracted to and bonded to the exterior of the primary cluster. Figure 5 shows the donor groupings N(19), N(17), O(7) and

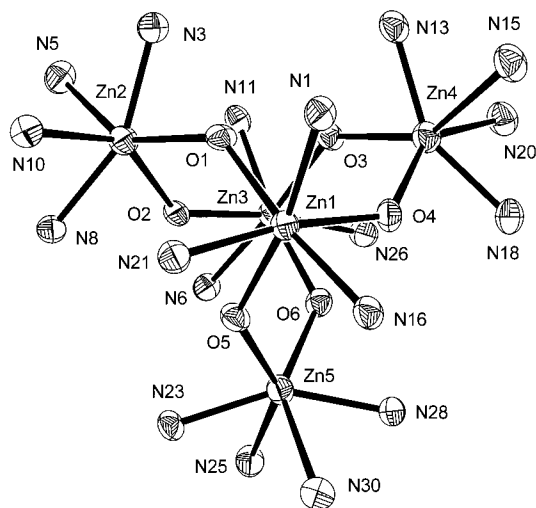


Figure 6. Core structural representation for $[\text{Zn}_5(\text{poap-H})_6](\text{ClO}_4)_4 \cdot 2.5\text{H}_2\text{O}$ (**4**) (40% probability thermal ellipsoids).

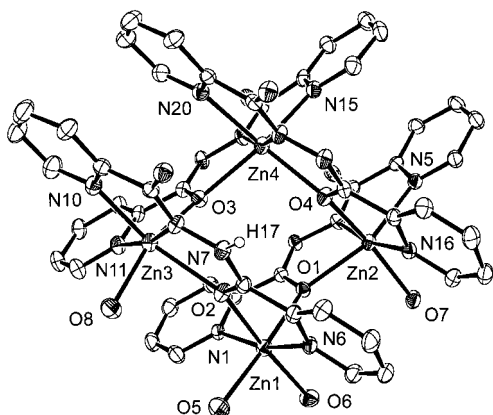


Figure 7. Structural representation of the cation in $[\text{Zn}_4(\text{poap})-(\text{Poap-H})_3(\text{H}_2\text{O})_4](\text{NO}_3)_5 \cdot 1.5\text{H}_2\text{O}$ (**5**) (40% probability thermal ellipsoids).

O(1), N(2), N(4) on two parallel ligands with the donor groupings suitably poised to possibly bind in a tridentate chelating fashion to additional metal centers. If all such external sites were occupied by metals a cluster with a total of eleven metal ions would result. It is of significance to note that the incorporation of one extra metal has been achieved with the formation of a (4+1) pentanuclear Cu(II) complex of p3oap.¹¹ One additional metal is bound in an identical, external ligand pocket, outside a square core. Similar reactions are being explored with **3**.

4 has a similar trigonal bipyramidal structure to those observed for **1–3**, with six ligands surrounding a pentanuclear $\text{Zn}(\text{II})_5[\mu\text{-O}]_6$ core. The structure of the trigonal bipyramidal core in **4** is illustrated in Figure 6, and important bond distances and angles are listed in Table 3. The essential features of the structure are the same as in **1–3**, with averaged Zn–ligand distances that are closer to those in **1** than in the manganese complexes. The presence of four perchlorates in the structure indicates that each ligand behaves as a monoanion.

The zinc nitrate complex (**5**) has a square $[2 \times 2]$ grid structure, in complete contrast to **4**. The structural representation of the cation is shown in Figure 7, and important bond distances and angles are given in Table 4. Two pairs of parallel and eclipsed tetradentate ligands are coordinated above and below the square $\text{Zn}_4[\mu\text{-O}]_4$ pseudo planar grid core. The zinc ions are six-coordinate, and since each ligand only fills five metal coordination sites extra ligands are required. Four water molecules fill this role with two bound to Zn(1) and one each to Zn(2) and Zn(3). Zn–Zn distances along the edges of the square fall in the range 3.97–4.21 Å, and Zn–O–Zn angles fall in the range 133.9–138.7°, similar to the dimensions of related square structures with other metal ions.^{10,11} Pyridine nitrogen atom separations within parallel pairs

Table 3. Interatomic Distances (Å) and Angles (deg) in **4**

Zn1–O1	2.084(4)	Zn4–N15	2.448(6)
Zn1–O4	2.108(4)	Zn4–N18	2.008(6)
Zn1–O5	2.090(4)	Zn4–N20	2.353(6)
Zn1–N1	2.140(6)	Zn5–O5	2.152(4)
Zn1–N16	2.128(6)	Zn5–O6	2.132(4)
Zn1–N21	2.139(6)	Zn5–N23	2.009(6)
Zn2–O1	2.144(4)	Zn5–N25	2.336(6)
Zn2–O2	2.156(4)	Zn5–N28	2.017(6)
Zn2–N3	2.011(6)	Zn5–N30	2.378(6)
Zn2–N5	2.331(6)	Zn1–Zn3	5.028(3)
Zn2–N8	2.009(6)	Zn3–Zn4	3.876(2)
Zn2–N10	2.363(6)	Zn2–Zn3	3.950(2)
Zn3–O2	2.097(4)	Zn3–Zn5	3.910(3)
Zn3–O3	2.100(4)	Zn1–Zn5	3.915(2)
Zn3–O6	2.095(4)	Zn1–Zn4	3.926(3)
Zn3–N6	2.138(6)	N2–N3	1.406(8)
Zn3–N11	2.124(6)	N7–N8	1.392(8)
Zn3–N26	2.143(6)	N12–N13	1.403(8)
Zn4–O4	2.106(4)	N17–N18	1.402(8)
Zn4–O4	2.133(4)	N22–N23	1.395(8)
Zn4–N13	2.006(6)	N27–N28	1.391(8)
Zn1–O4–Zn4			135.60(19)
Zn1–O5–Zn5			134.7(2)
Zn3–O6–Zn5			135.3(2)
Zn1–O1–Zn2			134.30(19)
Zn2–O2–Zn3			137.2(2)
Zn3–O3–Zn4			134.31(19)

Table 4. Interatomic Distances (Å) and Angles (deg) in **5**

Zn1–O1	2.125(3)	Zn3–N11	2.111(3)
Zn1–O2	2.238(3)	Zn4–O3	2.232(3)
Zn1–O5	2.098(3)	Zn4–O4	2.176(3)
Zn1–O6	2.079(3)	Zn4–N13	2.010(3)
Zn1–N1	2.073(3)	Zn4–N15	2.228(3)
Zn1–N6	2.104(3)	Zn4–N18	2.023(3)
Zn2–O1	2.217(2)	Zn4–N20	2.279(3)
Zn2–O4	2.116(3)	Zn1–Zn2	4.063(1)
Zn2–O7	2.140(3)	Zn1–Zn3	4.204(1)
Zn2–N3	2.017(3)	Zn3–Zn4	3.984(1)
Zn2–N5	2.251(3)	Zn2–Zn4	3.977(1)
Zn2–N16	2.101(3)	N2–N3	1.399(4)
Zn3–O2	2.329(3)	N7–N8	1.393(4)
Zn3–O3	2.079(3)	N12–N13	1.398(4)
Zn3–O8	2.049(3)	N17–N18	1.390(4)
Zn3–N8	2.084(3)		
Zn3–N10	2.190(3)		
Zn1–O1–Zn2			138.66(12)
Zn1–O2–Zn3			133.98(11)
Zn3–O3–Zn4			135.04(13)
Zn2–O4–Zn4			135.79(13)

of ligands fall in a narrow range (3.6–3.84 Å), indicating very close approaches of the π orbitals of the aromatic rings, an essential feature of the alignment of this parallel ligand arrangement. Eight additional water molecules were found in the lattice structure.

A peculiar feature of this structure is the presence of five nitrate anions clearly identified in the lattice, and confirmed by elemental analysis on a dried sample. The most obvious implication of this is that one ligand is neutral, thus requiring five anionic ligands for a total charge balance. This is unprecedented with ligands of this sort, and so each ligand in the structure bears close scrutiny. One proton H(17) bonded to diazine nitrogen atom N(7) (Figure 7) was found in a difference map and refined, while no similar protons were located on equivalent nitrogen atoms on other ligands. This implies that this ligand is neutral. Other relevant data to support this include a very short carbonyl C=O bond (1.247(4) Å), compared with C–O single bonds in the other ligands (1.297(4) Å, 1.300(4) Å, 1.302(4) Å), single N–N bonds in all ligands (1.391–1.400 Å), and long Zn–O(2) contacts (2.329(3) Å, 2.238(3) Å) compared with others within the square, implying ligand neutrality at O(2).

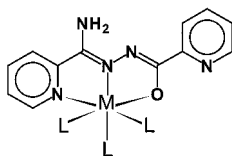


Figure 8. Putative precursor fragment for self-assembly process.

Discussion

Self-Assembly Processes. The design and synthesis of a polyfunctional, polytopic ligand, with the coordination pockets arranged appropriately such that on self-assembly in the presence of a metal ion a homoleptic cluster is produced, with an exact match between the coordination requirements of all the metals and the available ligand donor atoms, is not an easy task. Tetradentate ligands such as poap and its derivatives (Scheme 1) produce predominantly square, tetranuclear $M_4[\mu-O]_4$ ($M = \text{Mn(II)}, \text{Co(II)}, \text{Ni(II)}, \text{Zn(II)}, \text{Cu(II)}$) alkoxo-bridged grids using metal nitrates,^{10,11,29} with solvent molecules (e.g. H_2O) and occasionally nitrate anions occupying empty metal ion coordination sites. This arises because each ligand fills only five metal coordination positions, and these systems are not homoleptic.

The simplest homoleptic polynuclear cluster that can occur by a self-assembly process involves six ligands of this type and five metals (M_5L_6), with a thirty coordination site combination. On statistical grounds a pentanuclear cluster would seem much more likely than a higher oligomeric cluster, e.g., dodecanuclear. The formation of such a homoleptic system would of necessity require that serious donor competition from other prospective ligands be eliminated or reduced. The involvement of nitrate anions as ligands in the formation of some tetranuclear systems prompted us to use perchlorate salts instead, on the assumption that perchlorate is a much weaker donor than nitrate. Pentanuclear, trigonal bipyramidal, homoleptic clusters were successfully produced in high yield with some metal perchlorates in aqueous solvents (metal = $\text{Mn(II)}, \text{Co(II)}, \text{Zn(II)}$). The mechanism of self-assembly is difficult to assess, but appears not to involve the use of a weakly coordinated anion as a template, as has been observed in other cases,⁶ because the 'hole' within the square grid would be too small. Rather, pre-assembly of simpler, perhaps mononuclear subunits (e.g., Figure 8) probably precedes the final cluster formation, with self-assembly following a sequential docking procedure of the subunits. The extra ligands (L) will be either solvent molecules, e.g., water, or anions. If relatively strong donor anions (e.g. NO_3^- vs ClO_4^-) displace smaller solvent molecules, the process of docking of the preassembled subunits will be influenced by such ligands. The close approach of subunits necessary to form the homoleptic M_5 cluster would then be impeded, and it is reasonable that less crowded, e.g. tetranuclear, clusters would prevail. The unusual stoichiometry found for **5**, with one neutral ligand, may simply be a consequence of the solution pH during synthesis.

Thus far we have been successful in producing homoleptic M_5 complexes as the major products in the reaction of poap with $\text{Mn(II)}, \text{Co(II)}$ and Zn(II) perchlorates. Corresponding M_4 square complexes have not been isolated. In all cases the metal ions are six-coordinate, with pseudo-octahedral coordination geometries. While this situation prevails for poap, in the case of pzoapz (Scheme 1) a square complex $[\text{Co}_4(\text{pzoapz})_4(\text{H}_2\text{O})_4](\text{ClO}_4)_4 \cdot 3\text{H}_2\text{O}$ has been produced (50% yield),¹¹ indicating that in some cases oligomeric mixtures may be anticipated. It is significant that, so far, we have been unable to produce a Ni-

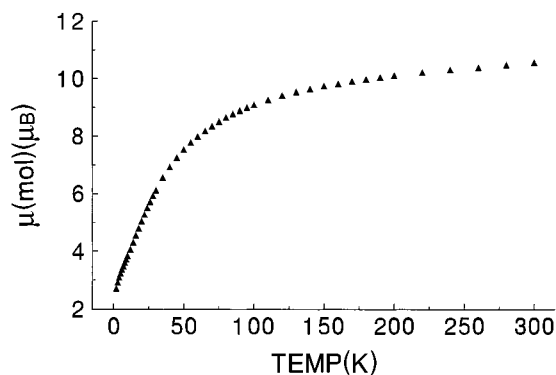


Figure 9. Magnetic data (μ_{mol}) (\blacktriangle) for **1** as a function of temperature.

(II)₅ trigonal bipyramidal cluster with ligands such as poap, even with Ni(II) perchlorate, which prefers to form a square tetranuclear grid complex with six-coordinate metal centers.¹⁰ There is also no evidence for the formation of pentanuclear trigonal bipyramidal copper(II) complexes with poap or any of its derivatives, and in all cases examined so far, regardless of the anion, complexes based on square or rectangular clusters are produced.^{10,11,28} This is probably associated with the usual desire of copper(II) for square or square-pyramidal geometries, and the six-coordinate environments imposed by the M_5L_6 arrangement are comparatively not as stable.

Magnetism. Variable temperature (2–300 K) magnetic susceptibility measurements were obtained for powdered samples of **1–3** in fields in the range 0.1–0.5 T. A plot of magnetic moment per mole for **1** is shown in Figure 9. The value drops from $10.6 \mu_B$ at 300 K to $2.7 \mu_B$ at 2 K, indicating significant antiferromagnetic coupling within the pentanuclear cluster. The low value at 2 K may indicate that the ground state for this system is $S = 1/2$. The room-temperature moment is consistent with the presence of five high spin Co(II) centers. No attempt has been made to fit these data to an isotropic Co(II)_5 trigonal bipyramidal exchange model.

Magnetic data for **2** and **3** follow a similar profile to **1** with a drop from $13.4 \mu_B$ (mol) at 300K to $5.8 \mu_B$ at 5 K (**2**), and from $12.9 \mu_B$ at 300K to $6.0 \mu_B$ at 4.5K (**3**). The room-temperature values in both cases are consistent with five high spin Mn(II) centers, and the drop with significant antiferromagnetic exchange within the cluster. The low-temperature values suggest a $S = 5/2$ ground state in both cases. The simple core arrangement of five Mn(II) centers linked by six almost equivalent alkoxo-bridges in the trigonal bipyramidal structure (Figure 4) would suggest a spin Hamiltonian with one J value of the following form (eq 1):

$$H = -J\{S_2 \cdot S_1 + S_2 \cdot S_3 + S_2 \cdot S_4 + S_5 \cdot S_4 + S_5 \cdot S_1 + S_5 \cdot S_3\} \quad (1)$$

$$\chi_M = \frac{N\beta^2 g^2}{3k(T - \theta)} \frac{\sum S_T(S_T + 1)(2S_T + 1)e^{-E(S_T)/kT}}{\sum S_T(2S_T + 1)e^{-E(S_T)/kT}} \quad (2)$$

$$\chi_M = \chi_M(1 - \rho) + \frac{2N\beta^2 g^2 \rho}{3kT} + \text{TIP} \quad (3)$$

Using the appropriate vector coupling scheme the appropriate energy levels and spin states were derived and substituted into the Van Vleck equation (eq 2), and corrections made for TIP (temperature independent paramagnetism), Weiss-like temperature effects (θ) and paramagnetic impurity fraction (ρ) (eq 3). The data for both **2** and **3** were fitted to eq 3 giving reasonable

(29) Thompson, L. K.; Matthews, C. J.; Xu, Z.; Zhao, J.; Parsons, S. R.; Heath, S. L. Unpublished results.

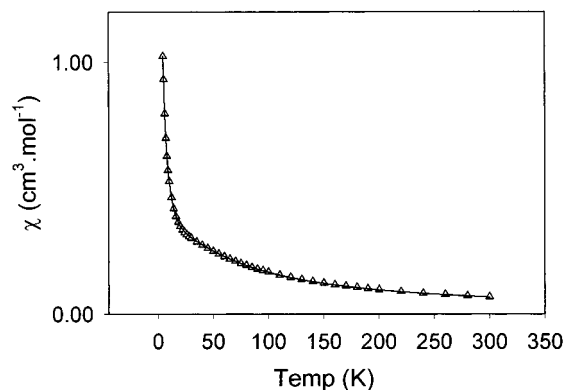


Figure 10. Magnetic data (χ_{mol}) (Δ) for **3** as a function of temperature (see text for fitting parameters).

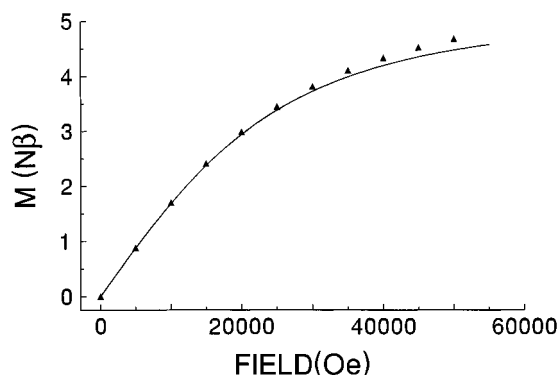


Figure 11. Magnetization data (\blacktriangle) as a function of field (Oe) at 4.5 K for **3**. The solid line represents the Brillouin function for $g = 2.03$, $S = 5/2$.

fits in both cases ($g = 2.02(1)$, $J = -1.8(2) \text{ cm}^{-1}$, $\text{TIP} = 10 \times 10^{-6} \text{ cm}^3 \cdot \text{mol}^{-1}$, $\rho = 0.002$, $\theta = -0.5 \text{ K}$ (**2**); $g = 2.002(5)$, $J = -1.5(1) \text{ cm}^{-1}$, $\text{TIP} = 0 \text{ cm}^3 \cdot \text{mol}^{-1}$, $\rho = 0.002$, $\theta = 0 \text{ K}$ (**3**)). Figure 10 shows experimental molar susceptibility as a

function of temperature for **3** and the theoretical line based on the above analysis. The negative J values indicate overall antiferromagnetic exchange within the clusters, consistent with the structure and the presence of short Mn–Mn spacings (3.85–4.05 Å) and large Mn–O–Mn bridge angles (125–132°). A comparable exchange integral ($J = -2.85 \text{ cm}^{-1}$) was observed for a $\text{Mn}_4(\mu_2\text{-O})_4$ square [2×2] grid complex of the ligand poapz (Scheme 1), which has comparable Mn–Mn separations (3.910(1) Å, 3.962(1) Å), and Mn–O–Mn angles (127.9°, 129.3°).¹¹ Magnetization data as a function of field for **3** at 4.5 K in the range 0–5 T are shown in Figure 11. The solid line represents the theoretical Brillouin function for a $S = 5/2$ system at 4.5 K ($g = 2.03$) consistent with the proposed ground state.

Conclusion

A series of novel, homoleptic, trigonal bipyramidal cluster complexes of Mn(II), Co(II) and Zn(II) is reported, which form by a strict self-assembly process with the ligands poap and p3oap and the appropriate metal perchlorate salt, such that there is an exact match between the coordination pockets presented by the cluster grouping of the ligands, and the coordination requirements of the cluster of five six-coordinate metal centers. The presence of a weakly coordinating anion (e.g., ClO_4^-) appears to be necessary to limit coordinative competition in the pre-assembly process, and the formation of the other possible oligomeric, nonhomoleptic tetranuclear square systems. In the zinc nitrate case the nonhomoleptic 2×2 square complex occurs as the only isolable self-assembly reaction product.

Acknowledgment. We thank NSERC (Canada) and EPSRC (UK) for financial support for this study, and Dr. R. McDonald (University of Alberta) for structural data.

Supporting Information Available: Crystallographic data in CIF format. This material is available free of charge via the internet at <http://pubs.acs.org>.

IC010301P